The Plant Journal (2000) **21**(2), 225–229

SHORT COMMUNICATION

Hyperpolarisation-activated calcium currents found only in cells from the elongation zone of *Arabidopsis thaliana* roots

Ed Kiegle, Matt Gilliham, Jim Haseloff and Mark Tester*
Department of Plant Sciences, University of Cambridge, Downing Street, Cambridge CB2 3EA, UK

Received 21 October 1999; revised 26 November 1999; accepted 2 December 1999.
*For correspondence (fax +44 1223 333 953; e-mail mat10@cus.cam.ac.uk).

Summary

Calcium currents across the plasma membrane of plant cells allow transduction of environmental signals as well as nutritive calcium uptake. Using transgenic *Arabidopsis* plants with cell-specific expression of green fluorescent protein (GFP), we analyzed whole cell calcium currents in epidermal cells of the rapidly growing root apex, mature epidermal cells, cortical and epidermal cells from the elongation zone, and mature pericycle cells. In cells only from the rapidly growing root apex, a hyperpolarisation-activated calcium current was identified. This current was irreversibly inhibited by 10 μM Al^{3+}, as well as being inhibited by 1 mM Co^{2+} and 100 μM verapamil. In no cells could a depolarisation-activated current be attributed to calcium influx. In the growing root apex, the hyperpolarisation-activated calcium current may function to allow constitutive uptake of calcium for rapid cell division and elongation.

Introduction

The role of plasma membrane Ca^{2+} influx in plant growth and development is twofold: it is required for signal transduction, and it is essential for cell division and expansion. To date, Ca^{2+} influx across the plasma membrane has been implicated in numerous signal transduction events, including responses to elicitors, cold and touch (Gelli *et al.*, 1997; Knight *et al.*, 1991). Little is known about the uptake pathway of rapidly growing plant tissues or the mechanisms of translocation of Ca^{2+} from the root to the shoot. One region of the root that is likely to require increased rates of Ca^{2+} uptake is the growing root apex. The root apex has significantly higher rates of cell division, cell elongation and Ca^{2+} uptake relative to the mature root (Beemster and Baskin, 1998; Huang *et al.*, 1992). We examined the dual role of Ca^{2+} uptake in *Arabidopsis* by examining differences in plasma membrane Ca^{2+} currents among several cell types in the mature and apical regions of roots.

Two types of plasma membrane Ca^{2+} currents have been identified in plant cells: a depolarisation-activated Ca^{2+} current, and a hyperpolarisation-activated Ca^{2+} current. The depolarisation-activated current has been described in some detail by direct and indirect methods (reviewed by White, 1998). In particular, the whole-cell patch clamp technique was applied to carrot suspension cells and *Arabidopsis* root cells, and Ca^{2+} currents that activated upon depolarisation, with a maximum between –75 mV and –100 mV identified (Thion *et al.*, 1996; Thion *et al.*, 1998; Thuleau *et al.*, 1994a; Thuleau *et al.*, 1994b). A hyperpolarisation-activated Ca^{2+} current was identified in whole cell recordings of suspension cultured cells of tomato (Gelli and Blumwald, 1997), and shown to be activated at membrane potentials negative of –120 mV.

It is expected that different cells will have different types of Ca^{2+} channels, depending upon the functions of the cell, its resting membrane potential, and the role of Ca^{2+} influx in the cell. To investigate the distribution of Ca^{2+} channel types within one organ, we took advantage of enhancer trap lines of *Arabidopsis* with expression of green fluorescent protein (GFP) in the ER of specific cell types to probe the cell and tissue specificity of plasma membrane Ca^{2+} currents. However, in no cell types could we unequivocally identify a depolarisation-activated Ca^{2+} current – all depolarisation-activated currents observed were consistent with an efflux of SO_4^{2-}, as has been described recently by Frachisse *et al.* (1999). In cells only from the elongation zone of roots, a hyperpolarisation-activated current was identified that was inhibited irrever-

sibly by low concentrations of Al^{3+} (as well as higher concentrations of Co^{2+} and verapamil). The cell type specific localization of one Ca^{2+} uptake mechanism suggests a role for this channel in cell enlargement.

Results

Four lines of *Arabidopsis* were selected from a library of enhancer trap lines expressing GFP in the endoplasmic reticulum in a cell-type specific manner (Figure 1). Expression patterns were maintained in plants up to 4-weeks-old. Line J0481 showed epidermis-specific expression in both trichoblasts and atrichoblasts, with markedly brighter fluorescence in the root tips, which allowed selection of epidermal cells from the rapidly growing region of the root apex. Line Q2393 expressed GFP in the cortex and epidermis of the elongation zone, and J2661 expressed GFP in the mature pericycle. It was possible to identify cells expressing GFP after enzymatic digestion (Figure 1d).

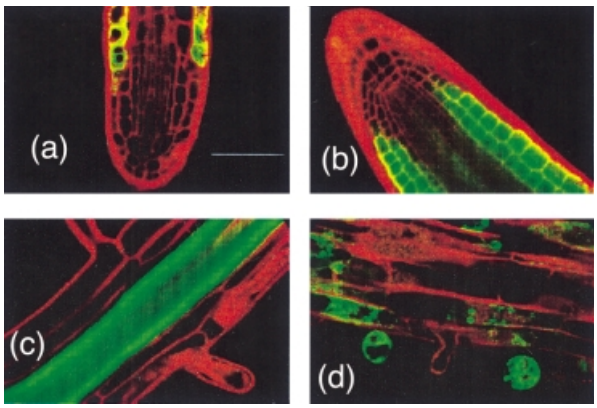

Figure 1. Cell specific expression of mGFP5 in roots stained with propidium iodide.
(a) J0481, expression in epidermal cells. (b) Q2393, expression in the elongation zone. (c) J2661, expression in mature pericycle. (d) Release of GFP-expressing epidermal protoplasts from the mature root of J0481 during enzymatic digestion. Scale bar = 50 μm.

In 43% of protoplasts from the cortex of the elongation zone (i.e. 9 out of 21), and 58% of protoplasts from the epidermis of the growing root tip (i.e. 14 out of 24), a hyperpolarisation-activated current was present (Figure 2a,b; Table 1). Although we observed this current in elongation zone cortical cells, the lower frequency and magnitude (average maximal current in cells displaying the hyperpolarisation-activated current was 37 ± 6 pA) of the current compared to that in apical epidermal cells (e.g. Figure 2a) reduces its contribution to average whole cell currents (Table 1). No recording from mature epidermal or pericycle protoplasts contained this type of current.

The hyperpolarisation-activated current was apparent immediately upon the formation of whole-cell configuration, and displayed slow voltage-dependant activation kinetics at holding potentials negative of –150 mV. Currents varied in magnitude from cell to cell, but they were not affected by depolarizing prepulses. This current was absolutely dependent on the presence of external

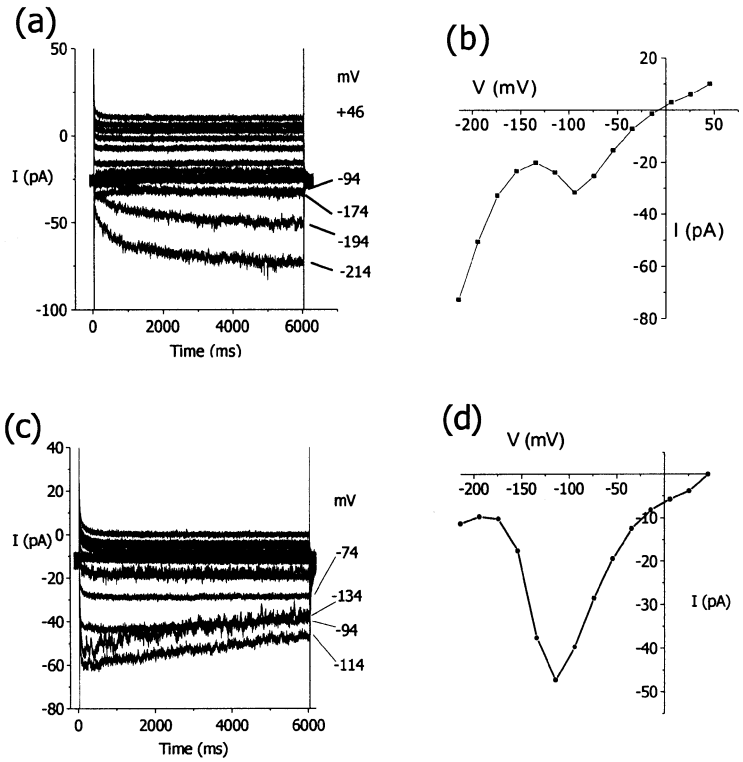

Figure 2. (a, b) Hyperpolarisation-activated Ca^{2+} currents in epidermal cells from the growing root tip.
(a) From a holding potential of –74 mV, currents evoked during steps from –214 mV to +46 mV in +20 mV steps, as described in Experimental procedures.
(b) I-V plot of the current after 6 sec at each voltage (i.e. at the end of the pulses shown in (a).
(c,d) Depolarisation-activated SO_4^{2-} currents in mature epidermal cells. (c) From a holding potential of –174 mV, currents evoked during steps as in (a). (d) I-V plot using currents at the end of the pulses shown in (c), as described in (b).

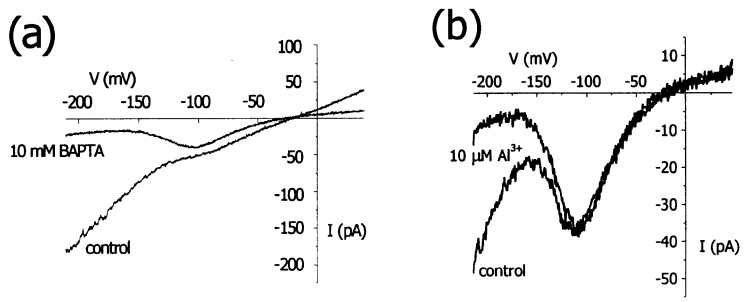

Figure 3. Inhibition of hyperpolarisation-activated currents from the root apex epidermis evoked during a 1 sec ramp from –214 to +64 mV [preceded by a 1 sec depolarising prepulse to +60 mV (a) or +106 mV (b)].
(a) Whole cell currents before and approximately 5 min after removal of all external Ca^{2+}.
(b) Whole cell currents before and approximately 1 min after addition of 10 μM Al^{3+} (bath pH = 4.5). The hyperpolarisation-activated Ca^{2+} current is irreversibly inhibited by Al^{3+}.

Table 1. Average currents across the plasma membrane of various root cell types at –214 mV (a voltage at which currents were dominated by the hyperpolarisation-activated Ca^{2+} current) and at −110 pA (where currents are dominated by a depolarisation-activated SO_4^{2-} current)

Cell type	I_{-214} (pA)	I_{-110} (pA)
Non-transformed (C24)	–26.5 ± 5	–62.6 ± 9
Mature pericycle (J2661)	–22.6 ± 3	–47.6 ± 9
Mature epidermis (J0481)	–29.7 ± 9	–44.9 ± 10
Root apex epidermis (J0481)	–44.2 ± 8	–52.8 ± 10
Elongation zone (Q2393)	–28.2 ± 6	–40.3 ± 9

Whole cell currents are presented as the mean ± SEM (n = 9–10).

Ca^{2+}, being abolished by the addition of 10 mM BAPTA (N = 5; see Figure 3a). Although hyperpolarization-activated currents reversed at potentials negative of the Ca^{2+} reversal potential (at approximately +100 mV), this is commonly seen with Ca^{2+} channels, due to the ready permeation through such channels of a range of other mono- and divalent cations (e.g. see Piñeros and Tester, 1995), a problem that can be made worse by apparent selectivities changing with ionic conditions (e.g. Piñeros and Tester, 1995; Allen and Sanders, 1994). In our solutions, the reversal potential could have been moved negative of E_{Ca} due to interaction of the channel with Mg^{2+} or TRIS (as well as Cl^- and SO_4^{2-}).

The sensitivity of the currents to channel antagonists was also consistent with them being due to Ca^{2+} influx. At 100 μM, the addition of Al^{3+} resulted in 87 ± 7% blockade of the hyperpolarisation-activated current and a similar result was seen with 100 μM La^{3+} and 1 mM Co^{2+}. Lower concentrations of Al^{3+} also greatly inhibited the hyperpolarisation-activated current (Figure 3b). Application of 100 μM verapamil completely inhibited the hyperpolarisation-activated component of whole-cell current. The similarity of the currents in the present work to those already characterized by Gelli *et al.* (1997) also supports our identification of these inward currents as being due to Ca^{2+} influx through Ca^{2+}-selective channels.

A depolarisation-activated current could also be observed in these cells, as well as in all other cell types studied (Figure 2c, d; Table 1). However, it was most likely that such currents were due to SO_4^{2-} efflux, rather than Ca^{2+} influx, as they were abolished by the removal of intracellular SO_4^{2-} and were not (or only weakly) sensitive to Ca^{2+} channel blockers at concentrations that inhibited the hyperpolarisation-activated current. Furthermore, currents remained upon complete removal of extracellular Ca^{2+} by BAPTA (Figure 3a). The currents could not be due to Cl^- efflux, as E_{Cl} was at –97 mV, not only well away from the reversal potential, but near the value for peak inward current. Interestingly, prepulses to positive potentials could often recruit these currents.

Recordings of cells randomly selected from protoplasts of non-fluorescent, wild-type C24 had similar properties to those of GFP-expressing cells from non-elongating tissues, with very low current at hyperpolarising potentials and the characteristic depolarisation-activated currents most likely to be attributable to SO_4^{2-} efflux.

Discussion

Calcium is a major component of all plant cells, found in high concentrations in most cellular compartments. Therefore, in roots of growing plants there is a need for large Ca^{2+} influxes to provide for the Ca^{2+} requirements of both expanding root cells and for delivery to the shoot. In the cytosol, however, the concentration of *free* Ca^{2+} is extremely low; thus, small changes in fluxes can lead to proportionately large changes in cytosolic free Ca^{2+} concentrations. This makes Ca^{2+} a useful ion for signal transduction, but could easily conflict with the needs of high Ca^{2+} fluxes for 'nutritional' purposes. These apparently opposing functions must require unique controls of Ca^{2+} transport in plant roots.

We have used plants with specific and localized expression of GFP, which allowed the identification and patch clamp analysis of specific root cell types after disruption of the intact root during protoplast formation (Maathuis *et al.*, 1998). Expression of GFP, when sequestered in the ER (Haseloff *et al.*, 1997), causes no evident disruption of plant growth and therefore cellular processes are likely to be largely unaltered.

We have shown the existence of a distinct hyperpolarisation-activated Ca^{2+} current in the roots of *A. thaliana*. A depolarisation-activated current was present in all cell types studied but, with the solutions we were using, it appeared most likely that this was due to the efflux of SO_4^{2-} through SO_4^{2-} permeable channels (Figure 3a; see also Frachisse *et al.*, 1999). The hyperpolarisation-activated Ca^{2+} current was found exclusively in expanding cells near the root apex. The presence of this current in expanding cells suggests it may have a role in the significant accumulation of Ca^{2+} essential for the growth of all plant cells.

Depolarisation-activated Ca^{2+} currents have been identified in carrot suspension cells and *Arabidopsis* root cells that could transduce environmental cues by allowing Ca^{2+} uptake when the membrane potential is shifted positive in response to a stimulus (Thion *et al.*, 1998; Thuleau *et al.*, 1994b). However, we were unable to observe similar currents in the material we used, even when using identical solutions and protocols to those used by Thion *et al.* (1998).

One physiological role of the hyperpolarisation-activated current in tomato suspension cells has been investigated previously with the patch clamp technique (Gelli *et al.*, 1997). Race-specific fungal elicitors stimulated this current. A pharmacological dissection implied a stimulatory role for G-proteins and phosphorylation in the activation of the channel. The inhibitor sensitivity of the hyperpolarisation-activated current in tomato suspension cells was very similar to that of *Arabidopsis* root protoplasts. The sensitivity of the hyperpolarisation-activated current in *Arabidopsis* root protoplasts to low concentrations of Al^{3+} is of particular interest, consistent with a central role of this influx pathway in root elongation and its inhibition by similar concentrations of Al^{3+} (compare, for example, Huang *et al.*, 1992). This result implies a central role for this channel in the mechanism of Al^{3+} inhibition of root elongation.

The localization of the hyperpolarisation-activated Ca^{2+} current in the growing root apex of *Arabidopsis*, a region with a high demand for Ca^{2+} uptake for cell division and cell expansion, leads us to postulate that it may also have a role in the 'nutritive' uptake of Ca^{2+} for growth and transport. We observed a similar, but larger, hyperpolarisation-activated current in cells from the endodermis (using line J3611), but the extreme difficulty of patch clamping this particular cell type has made more extensive analysis impossible.

With the use of the cell-specific GFP-expressing lines of *Arabidopsis*, we are now able to study the characteristics of Ca^{2+} channels in a range of cell types within roots, and thus provide insights into Ca^{2+} entry into plants for both signal transduction and nutrition.

Experimental procedures

Plant material/protoplast isolation

Plants from an enhancer trap library of *A. thaliana* C24 (Haseloff, unpublished) transformed with modified GFP (mGFP5ER) (Siemering *et al.*, 1996) were screened for expression in specific root cell types to produce the lines indicated in Figure 1. The lines are available from the Arabidopsis Stock Centers and are described at http://www.plantsci.cam.ac.uk/Haseloff/home.html. Plants were grown on 10 cm Petri dishes on sterile medium containing full strength Murashige and Skoog salts, 2% sucrose, and 0.8% agar under full spectrum fluorescent lights with 16 h days at 22°C. Roots from plants 7–14 days post-germination were screened on an epifluorescence microscope (see below) and excised. Protoplasts were released by digestion in a solution containing 10 mM KCl, 2 mM $CaCl_2$, 2 mM $MgCl_2$, 2 mM MES, 0.1% bovine serum albumin, 280 mM sorbitol, 2% Cellulase Onozuka RS (Yakult Honsha Co. Ltd, Tokyo, Japan), 1.2% Cellulysin (CalBiochem (U.K.) Ltd, Nottingham, UK), and 0.1% Pectolyase Y-23 (Seishin Corp., Tokyo, Japan), pH 5.5 (adjusted with KOH), for 1–3 h at 28°C. The protoplasts were purified by two centrifugations in Protoplast Control Bath (see below) at 200 ***g*** for 5 min. The protoplasts were resuspended in 1–2 ml of Protoplast Control Bath and stored on ice until use within 6 h.

Experimental solutions

Protoplast Control Bath contained 20 mM KCl, 2 mM $CaCl_2$, 2 mM $MgCl_2$, 10 mM 2-[N-Morpholino]ethanesulfonic acid (MES), pH 5.7 with KOH, $\pi_o = 280$ mOsm kg^{-1} with sorbitol. Bath solution contained 30 mM $CaCl_2$, 7 mM $CaSO_4$, 10 mM MES, 1 mM $MgSO_4$, pH 5.7 with Tris(hydroxymethyl)methylamine (TRIS), $\pi_o = 280$ mOsm kg^{-1} with ultrapure mannitol (Calbiochem) (Ca^{2+} activity = 12 mM). Calcium-free bath solution contained 60 mM tetraethylammonium (TEA)-Cl, 10 mM BAPTA, 10 mM MES, 1 mM $MgSO_4$, pH 5.7 (adjusted with TRIS), and π_o as previously. Pipette solution contained 10 mM N-hydroxyethylpiperazine N′-2-ethanesulfonic acid (HEPES), 10 mM TRIS-ATP, 5 mM TRIS-BAPTA, 5 mM $MgSO_4$, 2 mM $CaSO_4$, 0.5 mM $CaCl_2$, pH 7.2 (adjusted with TRIS), $\pi_o = 285$ mOskg^{-1} (adjusted with ultrapure mannitol; CalBiochem). The free Ca^{2+} was estimated to be 100–150 nM. Sulphate-free pipette solution contained 10 mM HEPES, 5.5 mM MgATP, 5 mM BAPTA, 3.6 mM Ca-glutamate, pH 7.2 (adjusted with TRIS), π_o as previously. The free Ca^{2+} was estimated to be 200 nM. ATP, BAPTA, $AlCl_3$ and verapamil were obtained from Sigma. Experiments with Al^{3+} were performed in bath solution of pH 4.5. As reported by Thuleau *et al.* (1994b), there was no significant effect on currents from changing the extracellular pH. All solutions were filtered through 0.22 μm filters (Millipore). Reversal potentials for ions in the solutions were calculated using ion activities estimated by GEOCHEM-PC.

Electrophysiology

Protoplasts were allowed to settle on a glass-bottomed chamber at 20°C and the whole cell patch clamp configuration was established as described previously (Roberts and Tester, 1995). The primary difference was the addition of Nikon epifluorescence attachments (FITC filter set) to a Diaphot 200 inverted microscope (Nikon U.K. Ltd, Surrey, UK) to visualize protoplasts expressing GFP. Pipettes were pulled from KIMAX51 glass and had a resistance of 10–15 MΩ. Whole cell currents were low-pass

filtered at 1–2 kHz and data were analyzed using the software package pClamp6 (Axon Instruments, Foster City, CA, USA) and Origin 5.0 with pClamp module (Microcal Software Inc., Northampton, MA, USA). Membrane potentials were corrected for measured liquid junction potentials. Cell surface area was calculated from whole-cell capacitance using a specific capacitance of 7.6 mF m^{-2} (Homann and Tester, 1997).

Voltage clamp protocols

To observe the time dependence of currents and to generate I-V relationships, 14 steps were generated from a holding potential (of either –74 mV or –214 mV, held for 3 sec between pulses) to –214 mV, –194 mV, and so on to +46 mV in +20 mV increments. In order to observe the kinetics of current activation, it is necessary to move from a holding potential at which the current is inactive to a holding potential at which the current is active. Thus, the activation kinetics of the depolarisation-activated current were observed by stepping from –214 mV, and the kinetics of the hyperpolarisation-activated current were observed by stepping from –74 mV. Current-voltage relations were made by plotting the apparent steady state current at the end of the 6 sec steps versus the holding potential during the step.

To measure recruitment and rapidly assay the inward currents, a ramp protocol was used. The membrane potential was held at –214 mV for 1 sec followed by a depolarizing prepulse (of –214 mV, –134 mV, –54 mV, +26 mV, or +106 mV) for 1 sec, then returning to –214 mV for 1 sec, before finally ramping voltage from –214 to +46 mV over 1 sec.

Confocal microscopy

Cell-specific expression of mGFP5 in the endoplasmic reticulum of the enhancer trap lines was imaged after staining living roots with propidium iodide (Sigma) using a laser-scanning confocal microscope (Bio-Rad, MRC 600) as described elsewhere (Berger *et al.*, 1998).

Acknowledgements

We would like to thank Anne Aliénor-Véry and Fouad Lemtiri Chlieh for technical advice, Sarah Hodge for the use of line Q2393, and The Royal Society and the BBSRC for funding to M.T.

References

Allen, G. and Sanders, D. (1994) Calcineurin, a type 2B protein phosphatase, modulates the Ca^{2+}-permeable slow vacuolar chanel of stomatal guard cells. *Plant Cell*, **7**, 1473–1483.

Beemster, G. and Baskin, T. (1998) Analysis of cell division and cell elongation underlying the developmental acceleration of root growth in *Arabidopsis thaliana. Plant Phys.* **116**, 1515–1526.

Berger, F., Linstead, P., Dolan, L. and Haseloff, J. (1998) Stomata patterning on the hypocotyl of *Arabidopsis thaliana* is controlled by genes involved in the control of root epidermis patterning. *Dev. Biol.* **194**, 226–234.

Frachisse, J.-M., Thomine, S., Colcombet, J., Guern, J. and Barbier-Brygoo, H. (1999) Sulfate is both a substrate and an activator of the voltage-dependent anion channel of Arabidopsis hypocotyl cells. *Plant Physiol.* **121**, 253–261.

Gelli, A. and Blumwald, E. (1997) Hyperpolarization-activated Ca^{2+}-permeable channels in the plasma membrane of tomato cells. *J. Mem. Biol.* **155**, 34–45.

Gelli, A., Higgins, V. and Blumwald, E. (1997) Activation of plant plasma membrane Ca^{2+}-permeable channels by race-specific fungal elicitors. *Plant Phys.* **113**, 269–279.

Haseloff, J., Siemering, K., Prasher, D. and Hodge, S. (1997) Removal of a cryptic intron and subcellular localization of green fluorescent protein are required to mark transgenic *Arabidopsis* plants brightly. *Proc. Natl Acad. Sci. USA*, **94**, 2122–2127.

Homann, U. and Tester, M. (1997) Ca^{2+}-independent and Ca^{2+}/GTP-binding protein-controlled exocytosis in a plant cell. *Proc. Natl Acad. Sci. USA*, **94**, 6565–6570.

Huang, J., Shaff, J., Grunes, D. and Kochian, L. (1992) Aluminum effects on calcium fluxes at the root apex of aluminum-tolerant and aluminum-sensitive wheat cultivars. *Plant Phys.* **98**, 230–237.

Knight, M., Campbell, A., Smith, S. and Trewavas, T. (1991) Transgenic plant aequorin reports the effects of touch and cold-shock and elicitors on cytoplasmic calcium. *Nature*, **352**, 524–526.

Maathuis, F., May, S., Graham, N., Bowen, H., Jelitto, T., Trimmer, P., Bennett, M., Sanders, D. and White, P. (1998) Cell marking in *Arabidopsis thaliana* and its application to patch-clamp studies. *Plant J.* **15**, 843–851.

Piñeros, M. and Tester, M. (1995) Characterization of a voltage-dependent Ca^{2+}-selective channel from wheat roots. *Planta*, **195**, 478–488.

Roberts, S. and Tester, M. (1995) Inward and outward K^+-selective currents in the plasma membrane of protoplasts from maize root cortex and stele. *Plant J.* **8**, 811–825.

Siemering, K., Golbik, R., Sever, R. and Haseloff, J. (1996) Mutations that suppress the thermosensitivity of green fluorescent protein. *Curr. Biol.* **6**, 1653–1663.

Thion, L., Mazars, C., Nacry, P., Bouchez, D., Moreau, M., Ranjeva, R. and Thuleau, P. (1998) Plasma membrane depolarization-activated calcium channels, stimulated by microtubule-depolymerizing drugs in wild-type *Arabidopsis thaliana* protoplasts, display constitutively large activities and longer half-life in *ton* 2 mutant cells affected in the organization of cortical microtubules. *Plant J.* **13**, 603–610.

Thion, L., Mazars, C., Thuleau, P., Graziana, A., Rossignol, M., Moreu, M. and Ranjeva, R. (1996) Activation of plasma membrane voltage-dependent calcium-permeable channels by disruption of microtubules in carrot cells. *FEBS Lett.* **393**, 13–18.

Thuleau, P., Moreau, M., Schroeder, J. and Ranjeva, R. (1994a) Recruitment of plasma membrane voltage-dependent calcium-permeable channels in carrot cells. *EMBO J.* **13**, 5843–5847.

Thuleau, P., Ward, J., Ranjeva, R. and Schroeder, J. (1994b) Voltage-dependent calcium-permeable channels in the plasma membrane of a higher plant cell. *EMBO J.* **13**, 2970–2975.

White, P. (1998) Calcium channels in the plasma membrane of root cells. *Ann. Bot.* **81**, 173–183.